

Dc Electrical Current Generated by Upstream Neutral Modes

Ankur Das,^{1,*} Sumathi Rao,^{2,3} Yuval Gefen,¹ and Ganpathy Murthy⁴

¹*Department of Condensed Matter Physics, Weizmann Institute of Science, Rehovot, 76100 Israel*

²*Harish-Chandra Research Institute, HBNI, Chhatnag Road, Jhansi, Allahabad 211 019, India*

³*International Centre for Theoretical Sciences (ICTS-TIFR), Shivakote, Hesarghatta Hobli, Bangalore 560089, India*

⁴*Department of Physics and Astronomy, University of Kentucky, Lexington, KY 40506, USA*

Quantum Hall phases are gapped in the bulk but support chiral edge modes, both charged and neutral. Here we consider a circuit where the path from the source of electric current to the drain necessarily passes through a segment consisting solely of neutral modes. We find that upon biasing the source, a dc electric current is detected at the drain, provided there is backscattering between counter-propagating modes under the contacts placed in certain locations. Thus, neutral modes carry information that can be used to nonlocally reconstruct a dc charge current. Our protocol can be used to detect any neutral mode that counterpropagates with respect to all charge modes. Our protocol applies not only to the edge modes of a quantum Hall system, but also to systems that have neutral modes of non-quantum Hall origin. We conclude with a possible experimental realization of this phenomenon.

I. INTRODUCTION

The quantum Hall effects (QHE)¹ are the earliest known example of topological insulators². They have a charge gap in the bulk, and all currents are carried by edge/surface modes, which can be either charged (with fractional charge in the fractional QHE) or neutral chiral modes. While the charge modes produce quantized electrical conductance, neutral modes are a manifestation of topology, electron-electron interactions, and possibly disorder, and contribute to heat transport. Neutral edge modes in quantum Hall systems have been detected by shot noise experiments³ and also by their quantized heat transport coefficients^{4,5}. Apart from quantum Hall systems, neutral (e.g. Goldstone) modes arise in systems in which a continuous symmetry is broken spontaneously.

In this work, we design a geometry where the unique current path from the source to the drain is forced to pass through a segment consisting of neutral modes only. We assume that the $U(1)$ symmetry of each channel is broken by the contacts; thus backscattering between channels is present under them. The breaking of these $U(1)$ symmetries results in a non-zero dc current at the drain. This protocol can be used either as a transformer, which converts charge current to neutral current, and then back to charge current, or as an efficient detector of neutral modes as long as the neutral counterpropagates with respect to all charge modes.

The proposed geometry is shown in Fig. 1. The relevant physics can be extracted by focusing on regions II, III, and IV. The solid black line at the top is a right-moving chiral charge mode, arising from a $\nu = 1$ quantum Hall system extending above Fig. 1, constituting the “probe” system. The dashed lines at the bottom in region III are a pair of counter-propagating gapless, bosonic⁶, neutral modes, presumed to arise from a “test” system extending below Fig. 1. The test system may be quantum Hall, so long as all its charge modes (dash-dotted orange lines) are right-moving, or it may be a system

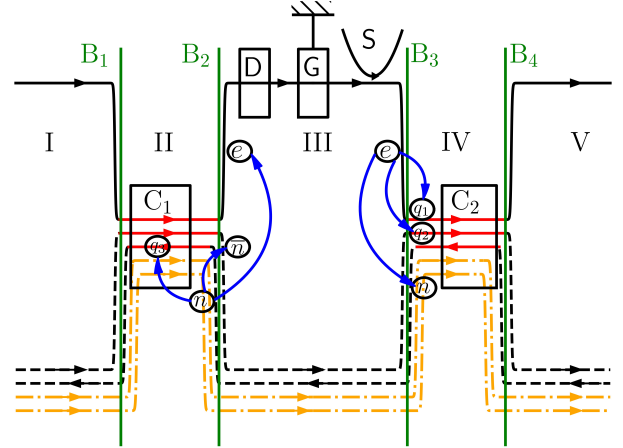


FIG. 1. A single right-moving chiral charged mode (solid black line) represents the edge of a $\nu = 1$ quantum Hall system extending above the figure, which is the “probe” system. Charges are injected at the source S and detected at the drain D . The “test” system extends below the figure, and has two counterpropagating neutral modes (dashed black lines), and possibly other charged chiral modes (dash-dotted orange lines), which all have to be right-moving for our scheme to be relevant. The edges of the two systems overlap only in regions II and IV, separated from the active region III by boundaries B_2 , B_3 . Density-density interactions between the chiral modes of the top and bottom systems exist only in regions II and IV, which also host the contacts C_1 and C_2 . Regions I and V are present to specify boundary conditions. Tunneling/scattering between the chiral modes occurs solely under the contacts. Reflection and transmission of a right-moving charge injected at S is shown schematically at B_3 , while a similar process for a left-moving neutral excitation is shown at B_2 .

with neutral modes only, such as an XXZ chain. Electrons are injected from the source S via tunnelling into the probe chiral edge mode and detected at the drain D .

The source and drain are separated by a grounded contact G. Clearly, current cannot flow from S to D along the right-moving, chiral top edge. The edge modes of the probe and test systems overlap, and thus interact, only in regions II and IV. The interaction is of the density-density form, with separate number conservation in the “bare” charged and neutral modes. These interactions renormalize the bare charged and neutral modes such that, generically, all three renormalized eigenmodes have nonuniversal charge. Regions II and IV also host the contacts C_1 and C_2 respectively⁷, which we assume can be decoupled from the interacting modes at will. Finally, regions I and V are semi-infinite “free” regions, where the edges of the probe and test systems are fully decoupled and are present to fix the asymptotic boundary conditions.

Before proceeding we discuss the notion of ideal contacts. The latter refers to terminals connected to the edge modes, which absorb the entire impinging current with no detectable signal away from the contact⁸. Ideal contacts have been discussed in Refs. 7, 9–11 in the absence of interactions, and, in the presence of interactions, in 7, where it was shown that a microscopic realization of an ideal contact for counterpropagating edge modes requires backscattering between them.

Our results can be encapsulated in two ways: Firstly, neutral modes can carry information about the charge current, information that can be used to reconstruct the charge current at a different location. Secondly, one can use the charge chiral mode (top mode of Fig. 1) as a “probe”, and apply it to a “test” system (bottom of Fig. 1). In this functionality, our device can be used to detect coherently propagating bosonic⁶ neutral modes in the test system. A dc charge current at the drain is direct evidence for neutral modes.

More concretely, let us assume there is at least one left-moving neutral mode in the test system. When electrons are injected at the source S if both C_1 and C_2 are coupled to the modes in region II and IV respectively, a dc current will be detected at D, regardless of whether the test system has (right-moving) charge chirals or not. The presence of right moving chiral charge modes in the test system will not change this conclusion qualitatively.

Let us understand the physics in two extreme limits, when (i) both the contacts are coupled, or (ii) both of the contacts are decoupled.

Case (i) Both contacts coupled: Assuming no charge chiral modes in the test system, consider a charge (positive by fiat) injected into the probe chiral at S, which travels to the boundary B_3 . There, a lump of positive neutral density (a neutralon) is reflected into the left-moving neutral mode in region III and lumps of nonuniversal charge are transmitted into the two right-moving modes in region IV to be fully absorbed at C_2 . The left-moving neutralon in III travels to B_2 , at which point a positive (electrically) charged lump is reflected into the probe chiral, and an equal and opposite charge is transmitted into the left-moving mode in the region II,

to be fully absorbed at C_1 . There will also be a neutralon reflected into the right-moving neutral chiral in region III, which travels to B_3 . As usual, this will undergo transmission and reflection, with the transmitted part being completely absorbed at C_2 . The reflected neutralon part has the same sign as the original neutralon, and repeats the process described earlier with a smaller amplitude. With both contacts coupled, an infinite sequence of charge lumps *of the same sign* is detected at D. Thus, a dc current at S implies a dc current of the same sign (but with a nonuniversal magnitude) at D.

This is already an instance of the effect we are looking for. Now we add (right-moving) charge chirals to the test system. All proceeds as before until the left-moving neutralon impinges on B_2 . Now, in addition to the reflected neutral lump, charge lumps will be transmitted into the nonuniversal charge modes in region II (to be absorbed at C_1), and reflected into the probe and test charge chirals. The magnitude and sign of the charges are determined by the interaction parameters in region II. Recall that the reflection/transmission is deterministic because no tunneling between the different modes is involved. Thus, there is a dc current at D.

To summarize, when both contacts are coupled, if a left-moving neutral is present in the test system, there is always a dc current at D, as long as the charge chirals (if any) of the test system are all right-moving.

Case (ii) Both contacts decoupled: Initially, let us assume that no charge chiral modes are present in the test system. The first step (the injected lump of electric charge traveling from S to B_3 , resulting in the reflection of a neutralon and transmission of lumps of nonuniversal charge in the two right-moving chirals in region IV) is the same as before. However, now the right-moving lumps in region IV travel to B_4 and undergo repeated partial reflection and transmission. Similarly, the left-moving neutralon, upon arriving at B_2 , results in a charge lump in the probe charge chiral in III, and a left-moving charge lump in region II. This latter lump will undergo partial transmission/reflection at B_1 . This leads to multiple scattering at all the boundaries. However, we can assert, based on charge conservation, that *no dc current is observed at D*. Since no left-moving charge modes enter region III, the entire charge injected at S has to proceed to region V (after multiple scattering in region IV)¹². Any charge detected at D is initiated by a neutralon arriving at B_2 via the left-moving neutral in III and its descendants via multiple scattering. Since no total (time-integrated) charge enters region III from either of regions II or IV, the time-integrated charge entering the drain D must vanish. Evidently, charge noise will be detected at D. Similar logic ensures that the dc charge current exiting region IV into region V is the entire charge current injected at S.

These conclusions do not change when we allow (right-moving) charge modes in the test system. Since the interactions in regions II and region IV are density-density interactions, the total $U(1)$ “charge” (which is completely

independent of electric charge) of each mode has to be conserved in the dc limit. Thus, we conclude, that in the presence of (right-moving) charge chiral modes in the test system, we still need both the contacts to be coupled in order to have a non-zero current at the drain D.

In what follows, we will present an outline of the calculations leading to our results, relegating straightforward mathematical details to the supplemental material (SM¹³). For simplicity, we will focus on the case where the test system has neutral modes only.

We model the neutrals by an XXZ spin chain and the interaction between the spin chain and the spin-polarized charged mode as a spin-spin interaction. The model is described by the action in Eq. 1 where the probe charged mode is represented by the bosonic field ϕ_1 , the right-moving test neutral by ϕ_2 and the left-moving test neutral by ϕ_3 . The interaction between the neutrals ϕ_2 and ϕ_3 is denoted by $\lambda_{23}(x)$. The interaction between the charged mode and the spin chain, (the same for both the left- and right-moving neutrals), is denoted by $\lambda_{12}(x)$ ($=\lambda_{13}(x)$)

$$S = \frac{1}{4\pi} \int dx dt \left[-\partial_x \phi_1 (\partial_t \phi_1 + v_1 \partial_x \phi_1) - \partial_x \phi_2 (\partial_t \phi_2 + v_2 \partial_x \phi_2) + \partial_x \phi_3 (\partial_t \phi_3 - v_2 \partial_x \phi_3) - 2\lambda_{12}(x) \partial_x \phi_1 (\partial_x \phi_2 + \partial_x \phi_3) - 2\lambda_{23}(x) \partial_x \phi_2 \partial_x \phi_3 \right]. \quad (1)$$

Assuming the interactions are turned on abruptly in regions II and IV, we calculate the reflection ($r_{ij}^{B_\alpha}$) and transmission coefficients ($t_{ij}^{B_\alpha}$) at B_2 and B_3 , which allows us to compute the current at D as a function of time via multiple reflections¹².

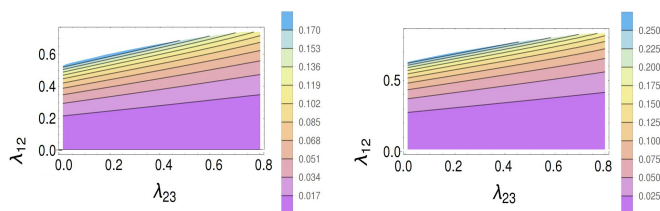


FIG. 2. The dc current at D as a function of the λ_{12} and λ_{23} for two different values of v_1, v_2 , when C_1, C_2 is coupled.

II. COMPUTATION OF CURRENT AND NOISE

When both C_1 and C_2 are coupled, the fraction of the current that reaches D as a function of time is

$$r_D(t) = r_{13}^{B_3} r_{31}^{B_2} \sum_{n=0}^{\infty} \left(r_{32}^{B_2} r_{23}^{B_3} \right)^n \delta(t - t_{d_n}) \quad (2)$$

where $t_{d_n} = t_0 + n\Delta t$. Here t_0 is the time for the first signal and Δt is the time for one full reflection between

B_3 and B_2 . The dc current at D is the zero-frequency limit of the Fourier transform.

$$I_D(\omega \rightarrow 0) = \frac{r_{13}^{B_3} r_{31}^{B_2}}{1 - r_{32}^{B_2} r_{23}^{B_3}} \langle I_{\text{tun}} \rangle \quad (3)$$

Similarly, we calculate the noise at D¹⁴⁻¹⁶ via the current-current correlation function on a Schwinger-Keldysh contour to obtain

$$N_D(\omega \rightarrow 0) = \frac{e(r_{13}^{B_3} r_{31}^{B_2})^2}{1 - (r_{32}^{B_2} r_{23}^{B_3})^2} \langle I_{\text{tun}} \rangle \quad (4)$$

The noise when one or both of the contacts are decoupled can be computed very similarly¹³.

When C_2 is decoupled the interactions in region IV are purely density-density, implying that the $U(1)$ “charge” of each mode (as previously mentioned, completely independent of electric charge) is conserved. Thus if we sum up all the multiple reflections from boundary B_3 and B_4 (dc limit), the total $U(1)$ “charge” of the neutral reflected from region IV to region III must vanish. Hence the total dc current at D will be zero. The dc current at the drain is only non-zero if and only if both the contacts C_1 and C_2 are coupled.

III. EXPERIMENTAL REALIZATION

We now discuss an experimental realization of our setup. For monolayer graphene, Hartree-Fock calculations suggest¹⁷ that at charge neutrality ($\nu = 0$), there is a quantum phase transition between a canted antiferromagnetic (CAF) phase, stabilized for purely perpendicular magnetic field, and a spin-polarized phase which can be stabilized by increasing the Zeeman energy E_Z with an in-plane B field. The spin-polarized phase has a fully gapped bulk and a pair of gapless helical edge modes^{18,19}, whereas the CAF phase breaks $U(1)$ spin-rotation symmetry and has a neutral Goldstone mode in the bulk, but no gapless charged edge modes^{20,21}. Experimentally, the phase transition has been seen²², but evidence that the phase at purely perpendicular B is the CAF phase is indirect, via the detection of magnon transmission above the Zeeman energy²³. Indeed, recent scanning tunneling spectroscopy measurements indicate that the ground state has bond-order²⁴⁻²⁶. To confirm that the system has CAF order one would need to detect *gapless* collective excitations, as has been done recently in bilayer graphene²⁷.

A potential experimental realization of the central idea of this paper is shown in Fig. 3. A sheet of graphene in a perpendicular B field is gated such that the left half is at filling $\nu = 1$, while the right half is at $\nu = 0$. In the central part of the $\nu = 0$ region, we overlay graphene with a ferromagnetic insulator, whose exchange field makes the graphene under it fully polarized and gapped. However, the annular periphery of $\nu = 0$ region is in the putative

CAF phase, with a gapless Goldstone mode. No topological edge modes exist between the two phases at $\nu = 0$. Confinement in the “radial” direction in the $\nu = 0$ region will reconstruct the continuum of bulk Goldstone modes into bands of clockwise-moving and anticlockwise-moving neutral modes. The lowest two bands will be gapless, and represent the counterpropagating neutral modes in Fig. 1. These counter-propagating neutral modes interact with the charge edge mode of the $\nu = 1$ quantum Hall phase on the left in the regions where they are proximate (Fig. 3). Adding the source S, drain D, and grounded contact G at appropriate locations realizes the setup of Fig. 1, and provides a way to unambiguously detect the gapless neutral Goldstone mode of the CAF.

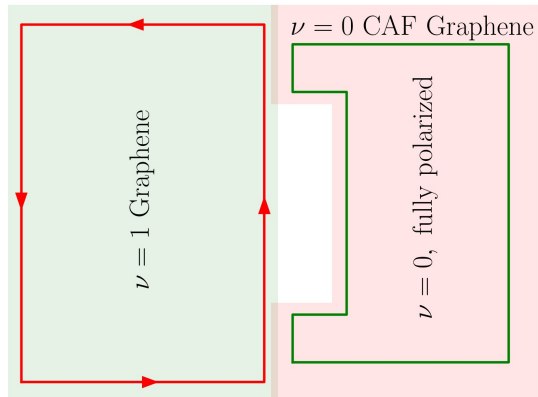


FIG. 3. A sheet of graphene in a perpendicular B -field is gated to have $\nu = 1$ on the left and $\nu = 0$ on the right. The central region of $\nu = 0$ is overlain by an insulating ferromagnet, inducing the fully polarized phase of $\nu = 0$ graphene in this region. The periphery of $\nu = 0$ is presumed to be in the CAF state, with gapless Goldstone modes. The lowest subband of the radially confined Goldstone modes interacts with the $\nu = 1$ edge mode and is detected by the scheme described in the text.

IV. SUMMARY AND OUTLOOK

In this work we have proposed a setup that has two functionalities: (i) Given a system known to have a neutral mode (the bottom system in Fig. 1), we encode information about the charge current into the neutral current, and subsequently read it out as a dc charge current at a different spatial location. (ii) Given a test system suspected of having coherently propagating, bosonic⁶, neutral modes, we place it along the bottom part of Fig. 1 and use our device as a neutral mode detector. An important condition for our protocol to work is that the neutral mode to be detected should counterpropagate with respect to all charge modes, else the charge modes will “short-circuit” the neutral mode. However, measurements of the upstream and downstream charge conductance along the edge of the test system are sufficient to

determine whether all charge modes co-propagate in a given system. Backscattering under the contacts breaks the $U(1)$ symmetry of each mode; without backscattering no dc current at the drain is possible.

Let us elaborate a bit on the functionality of our setup as a neutral mode detector. Our setup can detect coherently propagating, bosonic⁶, neutral edge modes when all the charge modes in the test system are gapped, and gapless modes represent spin/valley fluctuations. Trivial insulators with spontaneous symmetry breaking of a continuous symmetry, such as the putative CAF phase of graphene at charge neutrality, are prime examples of such systems. Moreover, our setup will detect coherently propagating, bosonic, neutral edge modes in QH systems as well, as long as two conditions are met: (i) all chiral charge modes of the test QH system are co-propagating, and (ii) there is at least one neutral mode which counter-propagates with respect to the charge modes. For example, the neutral mode of $\nu = 2/3$ at the Kane-Fisher-Polchinski fixed point²⁸ could be detected by our setup. Using monolayer graphene for the probe system allows one to reverse the propagation direction of the probe charge chiral *in situ* by gating to obtain $\nu = \pm 1$ in order to realize the geometry of Fig. 1. It must be noted that pairs of neutral edge modes can be generated by edge reconstructions in quantum Hall systems^{29,30}. We emphasize that our setup can detect coherently propagating bosonic neutral modes regardless of their physical origin.

Let us compare our setup with previous approaches to neutral mode detection. In one approach, the passage of upstream neutral modes through a quantum point contact was detected through the generation of charge noise^{3,31–33}. More recently, measurements of heat transport “upstream” as compared to charge transport have been employed^{34–36}. Not only are these hard measurements, (they require a precise determination of the temperature at a given contact), but they cannot determine whether the heat propagating upstream reflects coherent neutral modes rather than incoherent transport (e.g., due to diffusive modes). The latter is the result of charge and heat equilibration^{10,11}, and also leads to upstream charge noise³⁷.

A second theoretical approach for detecting neutral modes in certain quantum Hall systems^{38,39} via dc currents depends on tunneling between QH edges at quantum point contacts, and only specific neutral modes in specific configurations lead to dc currents. In our proposal, tunneling between different chiral modes occurs only under the contacts.

There are a few unresolved issues of broad import: (i) How does one understand the formulation of linear and non-linear response in the charge-neutral-charge circuit? (ii) Certain exotic spin systems are believed to have neutral Majorana modes^{40,41}, as is the $\nu = 5/2$ state³⁵. Our proposed device can detect bosonic⁶ neutral modes, but can some extension thereof be used to detect Majorana modes as well?

ACKNOWLEDGMENTS

We thank A. Mirlin, I. Gornyi, D. Polyakov, and K. Snizhko for their extremely valuable comments and proposed modifications which significantly improved our manuscript. AD was supported by the German-Israeli Foundation Grant No. I-1505-303.10/2019 and the GIF. AD also thanks Israel planning and budgeting committee (PBC) and Weizmann Institute of Science, Israel Dean of

Faculty fellowship, and Koshland Foundation for financial support. YG was supported by CRC 183 of the DFG, the Minerva Foundation, DFG Grant No. MI 658/10-1 and the GIF. SR and GM would like to thank the VAJRA scheme of SERB, India for its support. GM would like to thank the US-Israel Binational Science Foundation for its support via grant no. 2016130, and the Aspen Center for Physics (NSF grant PHY-1607611) where this work was completed.

- * ankur.das@weizmann.ac.il
- ¹ K. v. Klitzing, G. Dorda, and M. Pepper, *Phys. Rev. Lett.* **45**, 494 (1980), URL <https://link.aps.org/doi/10.1103/PhysRevLett.45.494>.
 - ² M. Z. Hasan and C. L. Kane, *Rev. Mod. Phys.* **82**, 3045 (2010), URL <https://link.aps.org/doi/10.1103/RevModPhys.82.3045>.
 - ³ A. Bid, N. Ofek, H. Inoue, M. Heiblum, C. L. Kane, V. Umansky, and D. Mahalu, *Nature* **466**, 585 (2010), ISSN 1476-4687, URL <https://doi.org/10.1038/nature09277>.
 - ⁴ V. Venkatachalam, S. Hart, L. Pfeiffer, K. West, and A. Yacoby, *Nature Physics* **8**, 676 (2012), ISSN 1745-2481, URL <https://doi.org/10.1038/nphys2384>.
 - ⁵ E. V. Deviatov, A. Lorke, G. Biasiol, and L. Sorba, *Phys. Rev. Lett.* **106**, 256802 (2011), URL <https://link.aps.org/doi/10.1103/PhysRevLett.106.256802>.
 - ⁶ By a bosonic mode we mean a chiral mode that can be described by a chiral boson living on the edge.
 - ⁷ C. Spånslätt, Y. Gefen, I. V. Gornyi, and D. G. Polyakov, *Phys. Rev. B* **104**, 115416 (2021), URL <https://link.aps.org/doi/10.1103/PhysRevB.104.115416>.
 - ⁸ C. L. Kane and M. P. A. Fisher, *Phys. Rev. B* **52**, 17393 (1995), URL <https://link.aps.org/doi/10.1103/PhysRevB.52.17393>.
 - ⁹ A. O. Slobodeniuk, I. P. Levkivskiy, and E. V. Sukhorukov, *Phys. Rev. B* **88**, 165307 (2013), URL <https://link.aps.org/doi/10.1103/PhysRevB.88.165307>.
 - ¹⁰ I. Protopopov, Y. Gefen, and A. Mirlin, *Annals of Physics* **385**, 287 (2017), ISSN 0003-4916, URL <https://www.sciencedirect.com/science/article/pii/S0003491617302142>.
 - ¹¹ C. Nosiiglia, J. Park, B. Rosenow, and Y. Gefen, *Phys. Rev. B* **98**, 115408 (2018), URL <https://link.aps.org/doi/10.1103/PhysRevB.98.115408>.
 - ¹² I. Safi and H. J. Schulz, *Phys. Rev. B* **52**, R17040 (1995), URL <https://link.aps.org/doi/10.1103/PhysRevB.52.R17040>.
D. L. Maslov and M. Stone, *Phys. Rev. B* **52**, R5539 (1995), URL <https://link.aps.org/doi/10.1103/PhysRevB.52.R5539>.
V. V. Ponomarenko, *Phys. Rev. B* **52**, R8666 (1995), URL <https://link.aps.org/doi/10.1103/PhysRevB.52.R8666>.
Y. Oreg and A. M. Finkel'stein, *Phys. Rev. B* **54**, R14265 (1996), URL <https://link.aps.org/doi/10.1103/PhysRevB.54.R14265>.
 - ¹³ Supplemental Material.
 - ¹⁴ T. Martin, Proceedings of the Les Houches Summer School, Session LXXXI (2005).
 - ¹⁵ C. d. C. Chamon, D. E. Freed, and X. G. Wen, *Phys. Rev. B* **51**, 2363 (1995), URL <https://link.aps.org/doi/10.1103/PhysRevB.51.2363>.
 - ¹⁶ E. Berg, Y. Oreg, E.-A. Kim, and F. von Oppen, *Phys. Rev. Lett.* **102**, 236402 (2009), URL <https://link.aps.org/doi/10.1103/PhysRevLett.102.236402>.
 - ¹⁷ M. Kharitonov, *Phys. Rev. B* **85**, 155439 (2012), URL <https://link.aps.org/doi/10.1103/PhysRevB.85.155439>.
 - ¹⁸ D. A. Abanin, P. A. Lee, and L. S. Levitov, *Phys. Rev. Lett.* **96**, 176803 (2006), URL <https://link.aps.org/doi/10.1103/PhysRevLett.96.176803>.
 - ¹⁹ L. Brey and H. A. Fertig, *Phys. Rev. B* **73**, 195408 (2006), URL <https://link.aps.org/doi/10.1103/PhysRevB.73.195408>.
 - ²⁰ G. Murthy, E. Shimshoni, and H. A. Fertig, *Phys. Rev. B* **90**, 241410 (2014), URL <https://link.aps.org/doi/10.1103/PhysRevB.90.241410>.
 - ²¹ G. Murthy, E. Shimshoni, and H. A. Fertig, *Phys. Rev. B* **93**, 045105 (2016), URL <https://link.aps.org/doi/10.1103/PhysRevB.93.045105>.
 - ²² A. F. Young, J. D. Sanchez-Yamagishi, B. Hunt, S. H. Choi, K. Watanabe, T. Taniguchi, R. C. Ashoori, and P. Jarillo-Herrero, *Nature* **505**, 528 (2014), ISSN 1476-4687, URL <https://doi.org/10.1038/nature12800>.
 - ²³ D. S. Wei, T. van der Sar, S. H. Lee, K. Watanabe, T. Taniguchi, B. I. Halperin, and A. Yacoby, *Science* **362**, 229 (2018), <https://science.sciencemag.org/content/362/6411/229.full.pdf>, URL <https://science.sciencemag.org/content/362/6411/229>.
 - ²⁴ S.-Y. Li, Y. Zhang, L.-J. Yin, and L. He, *Phys. Rev. B* **100**, 085437 (2019), URL <https://link.aps.org/doi/10.1103/PhysRevB.100.085437>.
 - ²⁵ X. Liu, G. Farahi, C.-L. Chiu, Z. Papic, K. Watanabe, T. Taniguchi, M. P. Zaletel, and A. Yazdani, *Science* **375**, 321 (2022), <https://www.science.org/doi/pdf/10.1126/science.abm3770>, URL <https://www.science.org/doi/abs/10.1126/science.abm3770>.
 - ²⁶ A. Coissard, D. Wander, H. Vignaud, A. G. Grushin, C. Repellin, K. Watanabe, T. Taniguchi, F. Gay, C. Winkelmann, H. Courtois, et al., *Imaging tunable quantum hall broken-symmetry orders in charge-neutral graphene* (2021), 2110.02811.
 - ²⁷ H. Fu, K. Huang, K. Watanabe, T. Taniguchi, and J. Zhu, *Phys. Rev. X* **11**, 021012 (2021), URL <https://link.aps.org/doi/10.1103/PhysRevX.11.021012>.

- ²⁸ C. L. Kane, M. P. A. Fisher, and J. Polchinski, Phys. Rev. Lett. **72**, 4129 (1994), URL <https://link.aps.org/doi/10.1103/PhysRevLett.72.4129>.
- ²⁹ U. Khanna, G. Murthy, S. Rao, and Y. Gefen, Phys. Rev. Lett. **119**, 186804 (2017), URL <https://link.aps.org/doi/10.1103/PhysRevLett.119.186804>.
- ³⁰ A. Saha, S. J. De, S. Rao, Y. Gefen, and G. Murthy, Phys. Rev. B **103**, L081401 (2021), URL <https://link.aps.org/doi/10.1103/PhysRevB.103.L081401>.
- ³¹ A. Bid, N. Ofek, M. Heiblum, V. Umansky, and D. Mahalu, Phys. Rev. Lett. **103**, 236802 (2009), URL <https://link.aps.org/doi/10.1103/PhysRevLett.103.236802>.
- ³² Y. Cohen, Y. Ronen, W. Yang, D. Banitt, J. Park, M. Heiblum, A. D. Mirlin, Y. Gefen, and V. Umansky, Nature Communications **10**, 1920 (2019), ISSN 2041-1723, URL <https://doi.org/10.1038/s41467-019-09920-5>.
- ³³ S. Biswas, A. Das, H. K. Kundu, Y. Gefen, and M. Heiblum, *in preparation*.
- ³⁴ A. Yacoby, M. Heiblum, H. Shtrikman, V. Umansky, and D. Mahalu, Semiconductor Science and Technology **9**, 907 (1994).
- ³⁵ M. Banerjee, M. Heiblum, A. Rosenblatt, Y. Oreg, D. E. Feldman, A. Stern, and V. Umansky, Nature **545**, 75 (2017), ISSN 1476-4687, URL <https://doi.org/10.1038/nature22052>.
- ³⁶ S. K. Srivastav, R. Kumar, C. Spånslätt, K. Watanabe, T. Taniguchi, A. D. Mirlin, Y. Gefen, and A. Das, Phys. Rev. Lett. **126**, 216803 (2021), URL <https://link.aps.org/doi/10.1103/PhysRevLett.126.216803>.
- ³⁷ C. Spånslätt, J. Park, Y. Gefen, and A. D. Mirlin, Phys. Rev. Lett. **123**, 137701 (2019), URL <https://link.aps.org/doi/10.1103/PhysRevLett.123.137701>.
- ³⁸ D. E. Feldman and F. Li, Phys. Rev. B **78**, 161304 (2008), URL <https://link.aps.org/doi/10.1103/PhysRevB.78.161304>.
- ³⁹ J. Cano and C. Nayak, Phys. Rev. B **90**, 235109 (2014), URL <https://link.aps.org/doi/10.1103/PhysRevB.90.235109>.
- ⁴⁰ A. Kitaev, Annals of Physics **321**, 2 (2006), ISSN 0003-4916, january Special Issue, URL <https://www.sciencedirect.com/science/article/pii/S0003491605002381>.
- ⁴¹ Y. Kasahara, T. Ohnishi, Y. Mizukami, O. Tanaka, S. Ma, K. Sugii, N. Kurita, H. Tanaka, J. Nasu, Y. Motome, et al., Nature **559**, 227 (2018), ISSN 1476-4687, URL <https://doi.org/10.1038/s41586-018-0274-0>.

Supplement to Dc Electrical Current Generated by Upstream Neutral Modes

Ankur Das,^{1,*} Sumathi Rao,² Yuval Gefen,¹ and Ganpathy Murthy³

¹*Department of Condensed Matter Physics, Weizmann Institute of Science, Rehovot, 76100 Israel*

²*Harish-Chandra Research Institute, HBNI, Chhatnag Road, Jhansi, Allahabad 211 019, India*

³*Department of Physics and Astronomy, University of Kentucky, Lexington, KY 40506, USA*

Here we describe the details of the calculation in supplement to the main text.

In this set of supplemental materials, we provide details of the action (Section SI), how the reflection and transmission coefficients are computed (Section SII), and how the current and the current noise at the drain are computed (Section SIII). While most of our analysis is in the case when the test system contains neutral modes only, we also analyze (Section SIV) an interesting special case when the “test” system (bottom of Fig. 1 in the main text) is the fractional quantum Hall state at $\nu = 2/3$, and thus has charge as well as neutral edge modes.

SI. ACTION AND EIGENMODES

In this section, we present details of the case considered in the main text, which assumes that there are no charge modes in the test system.

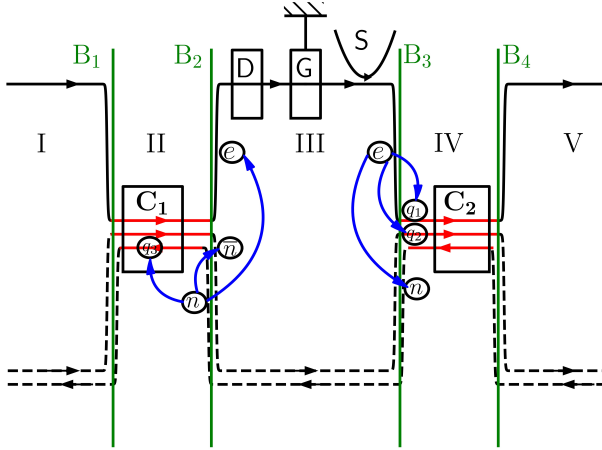


FIG. S1. The geometry of our detector, for the case, when the test system has no charge chiral edge modes. In regions II and IV there are density-density interactions between the test charge chiral and the test neutral chirals. C_1 and C_2 are perfect ohmic contacts while S , D are the source and drain separated by the grounded contact G .

The action corresponding to our model in Fig. S1 is

$$S = \frac{1}{4\pi} \int dx dt \left[-\partial_x \phi_1 (\partial_t \phi_1 + v_1 \partial_x \phi_1) - \partial_x \phi_2 (\partial_t \phi_2 + v_2 \partial_x \phi_2) + \partial_x \phi_3 (\partial_t \phi_3 - v_2 \partial_x \phi_3) - 2\lambda_{12}(x) \partial_x \phi_1 (\partial_x \phi_2 + \partial_x \phi_3) - 2\lambda_{23}(x) \partial_x \phi_2 \partial_x \phi_3 \right]. \quad (S1)$$

where we model the neutrals by an XXZ spin chain. Here ϕ_1 is the charge mode, ϕ_2 is the right-moving neutral mode and ϕ_3 is the left-moving neutral mode. The interaction between the neutrals, denoted by $\lambda_{23}(x) = \lambda_{23}$, is a constant everywhere. The interaction parameters between the charged mode and the neutral spin chain modes are $\lambda_{12}(x) (= \lambda_{13}(x))$, and are nonzero only in regions II and IV, and switch on abruptly at the boundaries of regions II and IV.

We define eigenmodes in each region, depending on the interaction strengths, as a linear combination of the bare modes. In regions where the test charged chiral mode is coupled (regions of II and IV) we write the bare fields ϕ_α^i in terms of the eigenmodes of Eq. S1 $\tilde{\phi}_\alpha^i$ as,

$$\phi_\alpha^i = M_{\alpha\beta} \tilde{\phi}_\beta^i. \quad (S2)$$

Similarly for region $j = I, III$ we can write the bare fields in terms of the eigenmodes ($\tilde{\phi}_\beta^j$) as,

$$\phi_\alpha^j = N_{\alpha\beta} \tilde{\phi}_\beta^j. \quad (S3)$$

We will use these definitions to calculate the reflection and transmission coefficients at every boundary. The matrix N depends on a single parameter because only the two bare neutral modes of the test system are mixed. However, the matrix M is more complex, and can be written as a real member of the group $SO(2,1)$. More explicitly,

$$M = \begin{bmatrix} 1 & 0 & 0 \\ 0 & \cosh(\xi_1) & \sinh(\xi_1) \\ 0 & \sinh(\xi_1) & \cosh(\xi_1) \end{bmatrix} \cdot \begin{bmatrix} \cosh(\xi_2) & 0 & \sinh(\xi_2) \\ 0 & 1 & 0 \\ \sinh(\xi_2) & 0 & \cosh(\xi_2) \end{bmatrix} \cdot \begin{bmatrix} \cos(\theta) & \sin(\theta) & 0 \\ -\sin(\theta) & \cos(\theta) & 0 \\ 0 & 0 & 1 \end{bmatrix} \quad (S4a)$$

$$N = \begin{bmatrix} 1 & 0 & 0 \\ 0 & \cosh(\xi) & \sinh(\xi) \\ 0 & \sinh(\xi) & \cosh(\xi) \end{bmatrix}. \quad (S4b)$$

The θ, ξ_i appearing in these matrices can be determined in a straightforward manner from the action.

* ankur.das@weizmann.ac.il

SII. FINDING REFLECTION AND TRANSMISSION

The equations of motion resulting from the action of Eq. S1 are

$$\frac{\partial^2 \phi_1}{\partial x \partial t} + v_1 \frac{\partial^2 \phi_1}{\partial x^2} + \frac{d}{dx} \left[\lambda_{12}(x) \left(\frac{\partial \phi_2}{\partial x} + \frac{\partial \phi_3}{\partial x} \right) \right] = 0 \quad (\text{S5a})$$

$$\frac{\partial^2 \phi_2}{\partial x \partial t} + v_2 \frac{\partial^2 \phi_2}{\partial x^2} + \frac{d}{dx} \left[\lambda_{12}(x) \frac{\partial \phi_1}{\partial x} + \lambda_{23} \frac{\partial \phi_3}{\partial x} \right] = 0 \quad (\text{S5b})$$

$$\frac{\partial^2 \phi_3}{\partial x \partial t} - v_3 \frac{\partial^2 \phi_2}{\partial x^2} - \frac{d}{dx} \left[\lambda_{12}(x) \frac{\partial \phi_1}{\partial x} + \lambda_{23} \frac{\partial \phi_3}{\partial x} \right] = 0. \quad (\text{S5c})$$

For future convenience, we have kept the notations v_2 and v_3 , though for the purposes of this section $v_2 = v_3$. Fourier transforming them to the frequency domain results in the following equations.

$$-i\omega \phi'_1 + v_1 \phi''_1 + [\lambda_{12}(x) (\phi'_2 + \phi'_3)]' = 0 \quad (\text{S6a})$$

$$-i\omega \phi'_2 + v_2 \phi''_2 + [\lambda_{12}(x) \phi'_1 + \lambda_{23} \phi'_3]' = 0 \quad (\text{S6b})$$

$$-i\omega \phi'_3 - v_3 \phi''_3 - [\lambda_{12}(x) \phi'_1 + \lambda_{23} \phi'_2]' = 0. \quad (\text{S6c})$$

Here prime represents derivative with respect to x . Now we integrate across the boundary, assuming ϕ_i to be continuous across it. This leads to the following boundary conditions across an arbitrary boundary where the interaction strengths change abruptly:

$$v_1 [\phi'_{10-}]^{0+} + [\lambda_{12}(x) (\phi'_2 + \phi'_3)]_{0-}^{0+} = 0 \quad (\text{S7a})$$

$$v_2 [\phi'_{20-}]^{0+} + [\lambda_{12}(x) \phi'_1 + \lambda_{23} \phi'_{30-}]^{0+} = 0 \quad (\text{S7b})$$

$$v_3 [\phi'_{30-}]^{0+} + [\lambda_{12}(x) \phi'_1 + \lambda_{23} \phi'_{20-}]^{0+} = 0. \quad (\text{S7c})$$

Here $0\pm$ represents across the boundary, and depending on the boundary, the values of λ_{ij} change.

A. Boundary type I

This type of boundary corresponds to the probe chiral not interacting with anything to the left, while it interacts with the test chirals on the right, as in the cases of boundaries B₁ and B₃. If the boundary is at $x = 0$ we have

$$\lambda_{12}(x) = \lambda_{12} \theta(x). \quad (\text{S8})$$

We now write the boundary conditions for the three incoming channels as

Case I: Source coming from the left through channel 1, i.e.

$$(\tilde{\phi}_1^j)' \Big|_{0-} = (\phi_1^j)' \Big|_{0-} = 1, \text{ and}$$

$$(\tilde{\phi}_2^j)' \Big|_{0-} = N_{2\beta}^{-1} (\phi_\beta^j)' \Big|_{0-} = 0 \quad (\text{S9a})$$

$$(\tilde{\phi}_3^i)' \Big|_{0+} = M_{3\beta}^{-1} (\phi_\beta^i)' \Big|_{0+} = 0 \quad (\text{S9b})$$

Using these boundary conditions with Eq. S7 we solve for the reflection and transmission coefficients. We will denote the transmission coefficient ($t_{\alpha,\beta}^{B_j}$) and reflection coefficients ($r_{\alpha,\beta}^{B_j}$) where the respective transmission and reflection happens from α mode to β mode at boundary B_j . We will use this notation from now on.

Case II: Source coming from the left through channel 2, i.e.

$$(\tilde{\phi}_2^j)' \Big|_{0-} = N_{2\beta}^{-1} (\phi_\beta^j)' \Big|_{0-} = 1 \text{ and}$$

$$(\tilde{\phi}_1^j)' \Big|_{0-} = (\phi_1^j)' \Big|_{0-} = 0 \quad (\text{S10a})$$

$$(\tilde{\phi}_3^i)' \Big|_{0+} = M_{3\beta}^{-1} (\phi_\beta^i)' \Big|_{0+} = 0 \quad (\text{S10b})$$

Case III: Source coming from the right through channel 3,

$$\text{i.e. } (\tilde{\phi}_3^i)' \Big|_{0+} = M_{3\beta}^{-1} (\phi_\beta^i)' \Big|_{0+} = 1 \text{ and}$$

$$(\tilde{\phi}_1^j)' \Big|_{0-} = (\phi_1^j)' \Big|_{0-} = 0 \quad (\text{S11a})$$

$$(\tilde{\phi}_2^j)' \Big|_{0-} = N_{2\beta}^{-1} (\phi_\beta^j)' \Big|_{0-} = 0 \quad (\text{S11b})$$

B. Boundary type II

In this type of boundary, the probe chiral interacts with the test chirals for $x < 0$, but does not interact for $x > 0$. Examples are B₂ and B₄, where we have

$$\lambda_{12}(x) = \lambda_{12} \theta(-x). \quad (\text{S12})$$

For this let us again write down different boundary conditions,

Case I: Source coming from the left through channel 1, i.e.

$$(\tilde{\phi}_1^j)' \Big|_{0-} = M_{1\beta}^{-1} (\phi_\beta^j)' \Big|_{0-} = 1 \text{ and}$$

$$(\tilde{\phi}_2^i)' \Big|_{0-} = M_{2\beta}^{-1} (\phi_\beta^i)' \Big|_{0-} = 0 \quad (\text{S13a})$$

$$(\tilde{\phi}_3^j)' \Big|_{0+} = N_{3\beta}^{-1} (\phi_\beta^j)' \Big|_{0+} = 0 \quad (\text{S13b})$$

Case II: Source coming from the left through channel 2, i.e.

$$(\tilde{\phi}_2^i)' \Big|_{0-} = M_{2\beta}^{-1} (\phi_\beta^i)' \Big|_{0-} = 1 \text{ and}$$

$$(\tilde{\phi}_1^j)' \Big|_{0-} = M_{1\beta}^{-1} (\phi_\beta^j)' \Big|_{0-} = 0 \quad (\text{S14a})$$

$$(\tilde{\phi}_3^j)' \Big|_{0+} = N_{3\beta}^{-1} (\phi_\beta^j)' \Big|_{0+} = 0 \quad (\text{S14b})$$

Case III: Source coming from the right through channel 3,

$$\text{i.e. } \left(\tilde{\phi}_3^j\right)' \Big|_{0+} = N_{3\beta}^{-1} \left(\phi_\beta^j\right)' \Big|_{0+} = 1 \text{ and}$$

$$\left(\tilde{\phi}_1^i\right)' \Big|_{0-} = M_{1\beta}^{-1} \left(\phi_\beta^i\right)' \Big|_{0-} = 0 \quad (\text{S15a})$$

$$\left(\tilde{\phi}_2^i\right)' \Big|_{0-} = M_{2\beta}^{-1} \left(\phi_\beta^i\right)' \Big|_{0-} = 0 \quad (\text{S15b})$$

III. CURRENT AND NOISE AT D

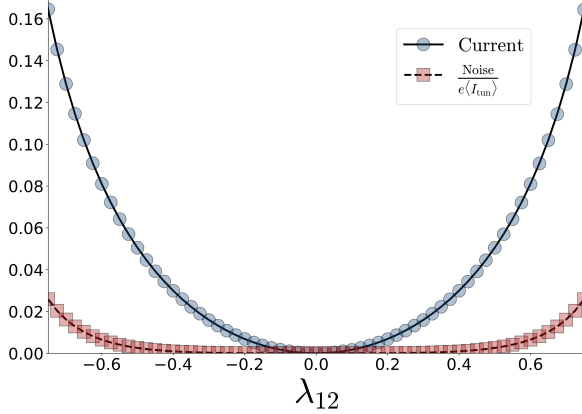


FIG. S2. Dc current and noise as a function of λ_{12} for $\lambda_{23} = 0.5$ for velocities $v_1 = 1.0$, $v_2 = 1.1$ when both contacts are coupled.

First let us consider the case when the C_1 and C_2 are both coupled. Because they are perfect contacts [1] they absorb all the currents (charge or neutral) that reach region II and IV respectively. We will calculate the total fraction of the current injected at the source S that reaches the drain D. Different paths between S and D can be classified by the number of reflections at the boundaries B_2 and B_3 (these two numbers have to be equal). The greater the number of reflections, the longer the time to reach the drain. Therefore, the total current fraction at D, as a function of time is,

$$r_D(t) = r_{13}^{B_3} r_{31}^{B_2} \sum_{n=0}^{\infty} \Delta_n \delta(t - t_n). \quad (\text{S16})$$

Here $\Delta_n = \left(r_{32}^{B_2} r_{23}^{B_3}\right)^n$ and

$$t_n = t_0 + n\Delta T, \quad (\text{S17})$$

with t_0 being the shortest time to reach the drain and ΔT being the total time for one set of reflections at B_2 and B_3 . Taking the Fourier transform, the current fraction at D as a function of ω is

$$r_D(\omega) = \frac{r_{13}^{B_3} r_{31}^{B_2}}{1 - r_{32}^{B_2} r_{23}^{B_3} e^{i\omega\Delta T}} \quad (\text{S18})$$

We can now easily calculate the fraction of average tunneling current reaching the drain by summing over the all the charge packets reaching the drain as the zero frequency limit of this expression.

$$\begin{aligned} f &= r_{13}^{B_3} r_{31}^{B_2} \left[1 + r_{32}^{B_2} r_{23}^{B_3} + \left(r_{32}^{B_2} r_{23}^{B_3}\right)^2 + \left(r_{32}^{B_2} r_{23}^{B_3}\right)^3 + \dots \right] \\ &= \frac{r_{13}^{B_3} r_{31}^{B_2}}{1 - r_{32}^{B_2} r_{23}^{B_3}} \end{aligned} \quad (\text{S19})$$

Next we compute the zero temperature noise following Ref. 2 for this problem.

$$L(t, t') = \langle I_D(t) I_D(t') \rangle + \langle I_D(t') I_D(t) \rangle - 2\langle I_D(t) \rangle \langle I_D(t') \rangle. \quad (\text{S20})$$

Using $I_D(t) = r_D(t) I_1(t)$ we can write,

$$L(t, t + \tau) = r_D(t) r_D(t + \tau) S(\tau), \quad (\text{S21})$$

with $S(\tau)$ being the conventional partitioning noise [2, 3]. Averaging over t we get the noise

$$N_D(\tau) = h(\tau) S(\tau) \quad (\text{S22})$$

$$\text{where } h(\tau) = \lim_{T \rightarrow \infty} \frac{1}{T} \int_0^T r_D(t) r_D(t + \tau) dt \quad (\text{S23})$$

$$\text{and } S(\tau) = \frac{e^2 \Gamma^2}{2\pi^2 a^2} \cos(V_0 \tau) \frac{2 \left(1 - \frac{v_1^2 \tau^2}{a^2}\right)}{\left(1 + \frac{v_1^2 \tau^2}{a^2}\right)^2}. \quad (\text{S24})$$

Here the average tunneling current is $\langle I_{\text{tun}} \rangle = \frac{e\Gamma^2 V_0}{2\pi^2 v_1^2}$, where Γ is the tunneling amplitude from the source into the probe charge chiral, V_0 is the potential difference between the source and the probe charge chiral, and a is the UV cutoff ($a \rightarrow 0$ being the UV limit) [2]. Note that the dimension of $N_D(\tau)$ is the same as that of $S(\tau)$. Therefore, $N_D(\tau)$ has the dimensions of current squared and $N_D(\omega)/\langle I_{\text{tun}} \rangle$ has the dimensions of charge. Now, using Eq. S16 we can simplify $h(\tau)$ as,

$$h(\tau) = \left(r_{13}^{B_3} r_{31}^{B_2}\right)^2 \sum_{n, n'=0}^{\infty} \Delta_n \Delta_{n'} \delta(\tau + (t_n - t_{n'})). \quad (\text{S25})$$

Thus the noise at zero frequency will be

$$N_D(\omega = 0) = \left(r_{13}^{B_3} r_{31}^{B_2}\right)^2 \sum_{n, n'=0}^{\infty} \Delta_n \Delta_{n'} S(t_{n'} - t_n) \quad (\text{S26})$$

Now, using the expression for $S(\tau)$ from Eq. S24 in the limit $V_0 \rightarrow 0$ (small voltage difference) and $a \rightarrow 0$ we can easily find,

$$N_D(\omega = 0) = \frac{e \left(r_{13}^{B_3} r_{31}^{B_2}\right)^2}{1 - \left(r_{32}^{B_2} r_{23}^{B_3}\right)^2} \langle I_{\text{tun}} \rangle. \quad (\text{S27})$$

Thus we can plot the noise to $e\langle I_{\text{tun}} \rangle$ ratio as a function of the interaction strength. We show one illustrative case in Fig. S2. When both contacts are coupled, noise is present at D but weak.

Next let us consider the case where the C_1 is coupled but C_2 is decoupled. Previously, when both contacts were coupled, all signals transmitted at B_3 were absorbed at C_2 . Now, with C_2 decoupled, there will be multiple reflections in region IV. However, since there is no tunneling in any region, the $U(1)$ “charge” of each mode will be conserved. Thus the total reflected “charge” of the neutral (including all possible multiple reflections) from region IV to region III will vanish. Thus the dc current at the drain D will be zero.

SIV. AN EXAMPLE WITH A CHARGED MODE IN THE TEST SYSTEM

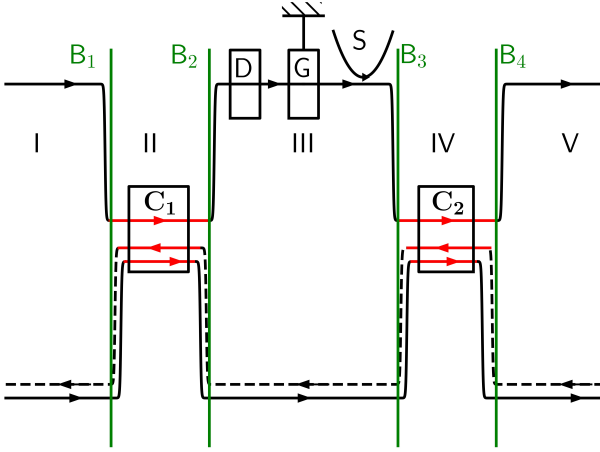


FIG. S3. A modified picture of the problem where the bottom region also has a right moving charged mode and a left moving neutral mode [4].

As we understand that in the absence of the contacts C_1 & C_2 there will be no current at the drain D due to the charge conservation. This also guarantees that the total current at D will be zero if we remove either of the contacts. However, we can again calculate the total current at D when both the contacts are coupled. The first packet that boundary B_3 via mode 1 will reflect back to mode 2 of region III with a fraction $r_{12}^{B_3}$. The part that transmits to region IV will get absorbed by C_2 . The packet that reflected into the mode 2 travels to boundary B_2 and one part reflects to mode 1 going towards the drain D with weight $r_{21}^{B_2}$, one part reflects to mode 3 travelling to boundary B_3 with weight $r_{23}^{B_2}$, and a part transmits to region II and gets absorbed by C_1 . The part that travelled to boundary B_3 will reflect back to mode 2 with weight $r_{32}^{B_3}$ and the same process as the previous step starts. Thus the fraction of total current reaching the drain will be a series with multiple reflection in region III

$$f = r_{12}^{B_3} r_{21}^{B_2} \sum_{n=0}^{\infty} \left(r_{23}^{B_2} r_{32}^{B_3} \right)^n = \frac{r_{12}^{B_3} r_{21}^{B_2}}{1 - r_{23}^{B_2} r_{32}^{B_3}}. \quad (\text{S28})$$

- [1] C. Spånslätt, Y. Gefen, I. V. Gornyi, and D. G. Polyakov, Phys. Rev. B **104**, 115416 (2021), URL <https://link.aps.org/doi/10.1103/PhysRevB.104.115416>.
 [2] T. Martin, Proceedings of the Les Houches Summer School, Session LXXXI (2005).
 [3] C. d. C. Chamon, D. E. Freed, and X. G. Wen, Phys. Rev.

- B **51**, 2363 (1995), URL <https://link.aps.org/doi/10.1103/PhysRevB.51.2363>.
 [4] C. L. Kane, M. P. A. Fisher, and J. Polchinski, Phys. Rev. Lett. **72**, 4129 (1994), URL <https://link.aps.org/doi/10.1103/PhysRevLett.72.4129>.